DALTON

Kinetic investigations into the copper(II)-catalysed peroxosulfate oxidation of Calmagite dye in alkaline media

John Oakes,* Gordon Welch and Peter Gratton

Unilever Research Port Sunlight Laboratory, Port Sunlight, Wirral, Merseyside, UK L63 3JW

Addition of Cu^{II} catalysed the peroxosulfate ($KHSO_5$) oxidation of Calmagite dye (D) in alkaline media and it was observed that the dye decomposition profiles exhibit extremely complex kinetic behaviour, with typical induction periods associated with rapid autocatalysis. A comprehensive kinetic model has been derived which not only can predict changes in speciation of reactants with time, but can also satisfactorily explain all the kinetic profiles. Much higher catalyst concentrations are required for copper(II) catalysis than for manganese(II) catalysis ($[KHSO_5] \gg [Cu^{II}] > [D]$ as opposed to $[KHSO_5] \gg [D] \gg [Mn^{II}]$), *i.e.* there needs to be excess Cu^{II} over D. This arises for two main reasons; first, binding of Cu^{II} to the dye inhibits its reaction with peroxosulfate, protecting the dye against oxidation, and secondly the active catalyst is a heterogeneous copper hydroxide species which arises when there is an excess of Cu^{II} in alkaline media. The unusual decomposition profiles are attributed to release of Cu^{II} into alkaline media *via* direct oxidation of the [CuD] complex by peroxosulfate. This oxidation is relatively slow, but when sufficient Cu^{II} is released 'true' autocatalysis is exhibited. The best simulated fits were obtained when the catalytic step was assumed to be first order in $[SO_5^{2-}]$ (*i.e.* peracid primarily acting as a nucleophile) and zero order in [CuD] as it is adsorbed onto the colloidal copper hydroxide.

The preceding paper[1] reported an investigation of the kinetics of the Mn^{II}-catalysed oxidation of Calmagite, a dye containing the *o*,*o*′-dihydroxy azo structural motif. In this paper the investigation is extended by including Cu^{II} as the metal catalyst. Copper(II) is reported to form only one complex with Calmagite,[2] having 1:1 stoichiometry, but it has a high stability constant ($\log K \approx 21$).

Although copper binds strongly to azo dyes[3] and peroxocopper complexes are known,[4] there is little reported scientific literature on the use of Cu^{II} for catalysing the oxidation of dyes in solution. Maybe this is not too surprising, since these investigations show the catalysis by Cu^{II} to be extremely complex, with typical decomposition profiles exhibiting induction periods, which precede rapid autocatalytic destruction of dye. As in the previous paper,[1] peroxosulfate ($KHSO_5$) is used as oxidant.

This paper outlines a combined kinetic, thermodynamic and spectroscopic investigation to elucidate the mechanism of Cu^{II}-catalysed oxidation of Calmagite. This has been facilitated by the design of a computer program to simulate not only reaction rates but also to calculate solution species and how these may vary as the reaction proceeds. A sophisticated fundamental approach of this nature is imperative to begin to unravel the complex chemistry of Cu^{II} in alkaline media and to attempt to answer key questions concerning (*a*) the nature of the active copper catalytic species, (*b*) the way [D] (D = dye) controls the reactivity of Cu^{II} and (*c*) whether the active oxidant species acts primarily as an electrophile or nucleophile.

At the outset it must be recognised that a key difference between these investigations and previous studies with Mn^{II} as catalyst is in the concentrations of catalyst employed for efficient catalysis. With manganese, $[D] \gg [Mn^{II}]$ and Calmagite is an efficient metal sequestrant, hence solution species are comparatively simple and there is a little background interference resulting from trace metal catalysis. On the other hand, in these studies $[Cu^{II}] > [D]$ so that a multiplicity of hydroxocopper species are present in alkaline media and kinetics can be influenced by indigenous trace metals. All these species need to be considered and the complexity arises from the need to incorporate numerous competing equilibria into the model.

A further difference is that dye oxidation is accompanied by catalysed oxidant decomposition. Decomposition of peracids proceeds *via* second-order kinetics and it is generally accepted that the uncatalysed reaction occurs by nucleophilic attack by the peracid anion upon the undissociated peracid.[5] Consequently, the observed rate exhibits a maximum at a pH equal to the pK_a of the peracid; similarly, this rate maximum is observed in the presence of trace metal impurities[6] (or in the presence of Cu^{II}) but rates are much higher.

Calmagite

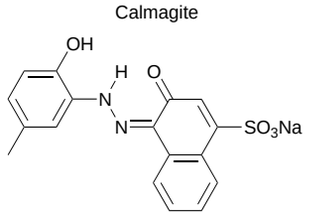

Methyl Orange

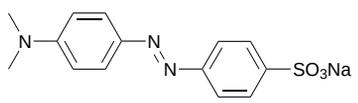

Results and Discussion

Complexation of Cu with Calmagite

Changes in the UV/VIS spectrum of Calmagite at pH 10 upon titration with Cu^{II} are shown in Fig. 1. The maximum shifts from 612 to 536 nm characteristic of a 1:1 complex, *via* an isosbestic point, representing a simple equilibrium between the two species. There was no evidence for a 2:1 complex.

Although the crystal structure of the [CuD] complex is unknown, that for the copper(II) complex of 1-(2-pyridylazo)-2-naphthol has been determined.[7] This forms a 1:1 complex which exhibits square-planar geometry; the dye is found to act as a tridentate ligand, with the *o*-pyridyl nitrogen, *o*-hydroxy oxygen and azo functions each directly co-ordinating to Cu^{II}, with solvent completing the co-ordination.

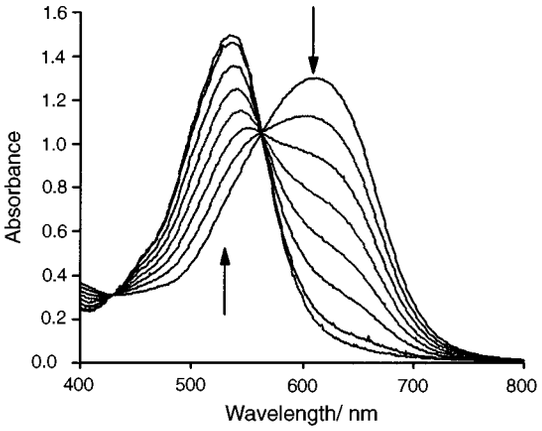

Fig. 1 Influence of Cu^{II} on the UV/VIS absorption spectrum of 6.5×10^{-5} M Calmagite at pH 10 and 40 °C. The dye peak at 612 nm is replaced by a peak at 536 nm upon titration with 1 mol equivalent of Cu^{II} added as 10 μM aliquots

Experimental observations

Unlike manganese(II) catalysis, the Cu^{II}-catalysed $KHSO_5$ oxidation of Calmagite depends critically upon [Cu^{II}]. The kinetic profiles for the $KHSO_5$ oxidation of Calmagite can be classified into three important regions, (I), (II) and (III).

(I) If kinetic studies are carried out under conditions where 'free' dye dominates the absorption spectrum (where [D] > [Cu^{II}]) no catalysis is observed, *i.e.* the rate constant obtained is identical to that for dye alone. There is no catalysis in this region since strong binding by the excess of Calmagite renders the copper inactive and dye oxidation can be understood simply in terms of direct oxidation of free Calmagite with peroxosulfate.

(II) When copper(II) levels are increased to approach those of the dye an induction period is exhibited, which results from the oxidation of 'free' dye prior to an extremely rapid reaction. This is illustrated in each of the reaction profiles shown in Fig. 2(*a*). It is clear that the magnitude of the induction period depends critically upon the ratio of dye to Cu^{II}. The onset of catalysed dye degradation is attributed to release of 'free' Cu^{II} due to oxidation of the copper–Calmagite complex [see (III)]. It is necessary to make this assumption since levels of 'free' Cu^{II} in equilibrium with [CuD] at its equivalence point (10^{-11} M) are too low to achieve significant catalysis. Under conditions of catalysis, speciation calculations outlined in the next section suggest that copper exists almost exclusively as a colloidal $Cu(OH)_2$ precipitate. Catalysed dye destruction is attributed to this species and in particular a high-surface-area intermediate occurring during its formation.

(III) Catalysis becomes significant under conditions where the 'free' dye spectrum becomes replaced by that of the [CuD] (where [Cu^{II}] > [D]). Indeed, the reaction speeds up as [D] decreases during the reaction, *i.e.* autocatalysis is exhibited [Fig. 3(*a*)]. Similarly, increasing the dye concentration decreases the rate. Under autocatalytic conditions effectively all the dye is complexed with copper so that loss in absorbance at 536 nm is due to direct oxidation of the bound dye, and not the 'free' dye with which it is in equilibrium, due to its insignificant concentrations.

Examination of $KHSO_5$ decomposition indicates that it follows the same trends as illustrated in Figs. 2(*a*) and 3(*a*) for oxidation of the dye; however, there is a slight difference as there is little $KHSO_5$ decomposition when dye is present and this decomposition only accelerates when dye loss becomes significant. In the presence of an excess of dye of [region (I)] no catalysed $KHSO_5$ decomposition is observed, which is consistent with the suggestion that when copper becomes complexed with Calmagite it is catalytically inert.

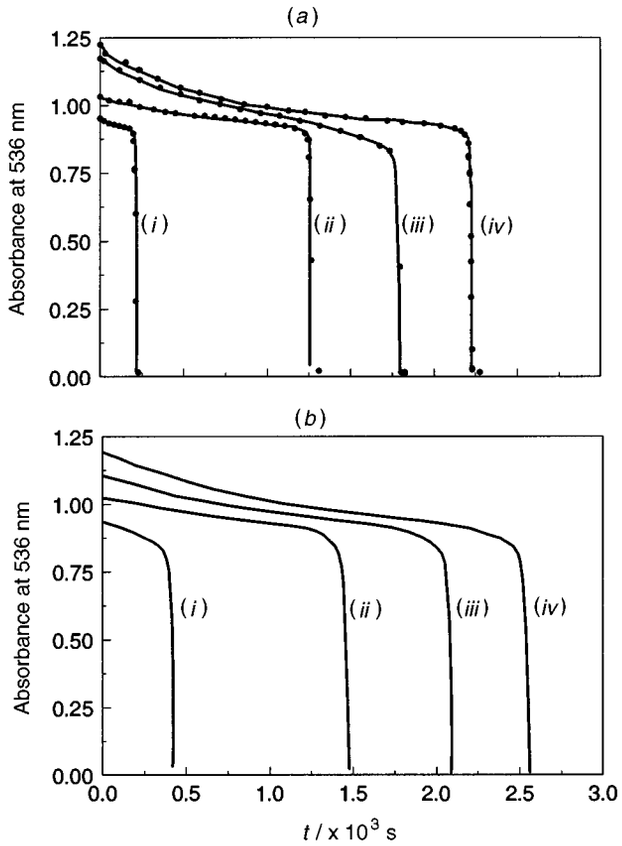

Fig. 2 (*a*) Change in absorbance of Calmagite with time upon catalysed oxidation with 1×10^{-3} M $KHSO_5$ using 3.9×10^{-5} M Cu^{II} at pH 10 and 40 °C. Curves (*i*) to (*iv*) correspond to $[D]_0 = 6 \times 10^{-5}$, 7×10^{-5}, 8×10^{-5} and 9×10^{-5} M, respectively. (*b*) Theoretical fits to the experimental data in (*a*)

Analysis of kinetic data

Computer modelling. In order to establish a credible reaction scheme for complicated kinetic processes it is necessary to calculate concentrations of species present in solution and to determine how these concentrations vary with time assuming various predetermined rate equations. These concentrations are converted into absorbances, using known absorption coefficients, and are compared to experimental results until a satisfactory simulation is achieved. To accomplish these comparisons we have used a finite difference model,[8] developed using independently generated constants and rate laws for constituent reactions of the scheme.

The finite difference method is a well developed technique for modelling time-dependent changes in complex systems. The first step in applying it to the Calmagite–Cu–$KHSO_5$ system is to calculate the state of the system at zero time. This requires knowledge of the initial concentrations of the reactants and estimates of the constants governing their equilibria. The model reaction is caused to move forward by a small interval of time; reaction occurs, products form and reactant concentrations decrease. An equilibrium state is calculated for the new system and another time interval is taken with further reaction. These steps are repeated until the required time has elapsed. The method is thus one of numerical integration. With this method it is possible to handle systems with large numbers of parallel and competitive reactions combined with complex equilibria. Different reaction schemes and equilibria can be added or subtracted very easily or changed at will. The time intervals should be so small that the use of smaller steps makes no significant difference to the computation.

Equilibria in the Calmagite–copper–peroxosulfate system. The interaction of Cu^{II} with Calmagite in the presence of $KHSO_5$ is

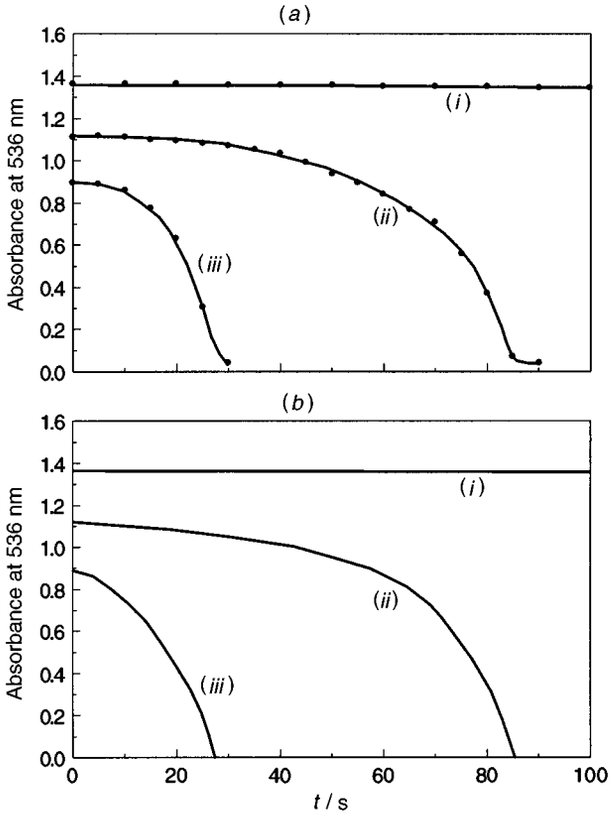

Fig. 3 (*a*) Change in absorbance of Calmagite with time upon catalysed oxidation with 5×10^{-4} M $KHSO_5$ using 6.3×10^{-5} M Cu at pH 10 and 40 °C. Curves (*i*) to (*iii*) correspond to $[D]_0 = 6.83 \times 10^{-5}$, 5.56×10^{-5} and 4.47×10^{-5} M, respectively. (*b*) Theoretical fits to the experimental data in (*a*)

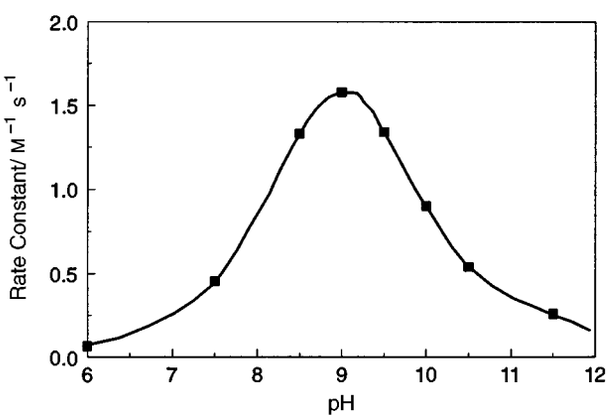

Fig. 4 Plot of observed second-order rate constant for the uncatalysed oxidation of 5×10^{-5} M Calmagite with 1×10^{-3} M $KHSO_5$ as a function of pH at 40 °C in the presence of 2×10^{-5} M ethylenedinitrilotetraacetate (edta). The solid line is the theoretical fit to the experimental points

complex, having numerous equilibria superimposed on the reaction scheme. Calmagite itself has two ionisable hydroxyl groups, equations (1) and (2). Copper binds to the doubly

$$H_2D \rightleftharpoons HD^- + H^+ \quad (pK = 8.4) \qquad (1)$$

$$HD^- \rightleftharpoons D^{2-} + H^+ \quad (pK = 12.7) \qquad (2)$$

deprotonated form, equation (3). Peroxosulfate has a similar set

$$[CuD] \rightleftharpoons Cu^{II} + D^{2-} \quad (pK = 21.8) \qquad (3)$$

of equilibria, (4) and (5). Copper ion forms a range of

$$HSO_5^- \rightleftharpoons SO_5^{2-} + H^+ \quad (pK = 9.5) \qquad (4)$$

$$[Cu(SO_5)] \rightleftharpoons Cu^{II} + SO_5^{2+} \quad (pK = 2.0) \qquad (5)$$

complexes with hydroxide ion and finally a precipitate of copper hydroxide, equations (6)–(10).

$$[Cu(OH)]^+ \rightleftharpoons Cu^{II} + OH^- \quad (pK = 6.6) \qquad (6)$$

$$Cu(OH)_2 \rightleftharpoons [Cu(OH)]^+ + OH^- \quad (pK = 12.8) \qquad (7)$$

$$[Cu(OH)_3]^- \rightleftharpoons Cu(OH)_2 + OH^- \quad (pK = 14.5) \qquad (8)$$

$$[Cu(OH)_4]^{2-} \rightleftharpoons [Cu(OH)_3]^- + OH^- \quad (pK = 15.6) \qquad (9)$$

$$Cu(OH)_2\ (ppt) \rightleftharpoons Cu^{II} + 2OH^- \quad (pK_{sp} = 19.3) \qquad (10)$$

These constants are obtained from standard compilations[2] and are mostly for ionic strengths of 0.1 M. The exceptions are pK_{sp}, the solubility product for $Cu(OH)_2$, which is at zero ionic strength and the constant for the Cu,SO_5^{2-} ion pair which is an estimate based on the value for the Cu,SO_4^{2-} ion pair. In fact, this constant is so low that it does not have a substantial influence on the system.

When dyes with structures similar to Calmagite are oxidised with enzymes *o*-naphthoquinone-type materials have been implicated as reaction products/intermediates[9] and these will also bind Cu^{II}. It is possible to assign values to these constants based on standard lists[2] for similar materials, equations (11)–(13).

$$HQ^- \rightleftharpoons Q^{2-} + H^+ \quad (pK = 12.1) \qquad (11)$$

$$H_2Q \rightleftharpoons HQ^- + H^+ \quad (pK = 8.2) \qquad (12)$$

$$[CuQ] \rightleftharpoons Cu^{II} + Q^{2-} \quad (pK = 12.0) \qquad (13)$$

Kinetics. The approach adopted in the analysis of the kinetics of the Cu^{II}–Calmagite–$KHSO_5$ system was to identify parts of the system which could be investigated in isolation and to derive the constants for these components using the finite difference method.

One such isolable reaction is the decolourisation of Calmagite by peroxosulfate in the absence of copper (Fig. 4). The reactions that occur are (14)–(16) where the peracid acts as an

$$H_2D + HSO_5^- \longrightarrow \text{products} \quad (0.7\ M^{-1}\ s^{-1}) \qquad (14)$$

$$HD^- + HSO_5^- \longrightarrow \text{products} \quad (2.0\ M^{-1}\ s^{-1}) \qquad (15)$$

$$D^{2-} + HSO_5^- \longrightarrow \text{products} \quad (1.6 \times 10^3\ M^{-1}\ s^{-1}) \qquad (16)$$

electrophile.[10] The values given for each reaction are the second-order rate constants. These constants give a good fit to changes in the observed rate constant with pH (Fig. 4). A full description of the kinetics of reaction between peracids and dyes will be given elsewhere.[10]

A second isolable reaction is catalysed oxidation. Insight into this reaction was obtained in the absence of dye but in the presence of added Cu^{II}. The measured second-order rate constants for the Cu^{II}-catalysed decomposition of $KHSO_5$ as a function of added Cu^{II} and in the absence of Calmagite are shown in Fig. 5. Despite considerable experimental scatter, typical of systems devoid of sequestrant, Fig. 5 reveals an atypical order in $[Cu^{II}]$. Initially, addition of Cu^{II} has only a small influence on $KHSO_5$ decomposition but its effect accelerates rapidly beyond a certain concentration. The line drawn in this figure is proportional to $[Cu^{II}]^2$.

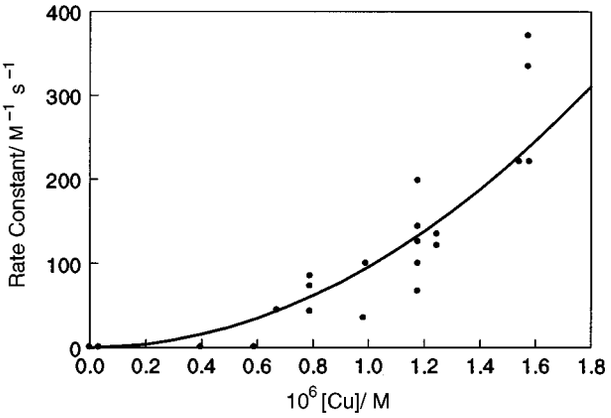

Fig. 5 Observed second-order rate constant for the catalysed decomposition of 5×10^{-4} M $KHSO_5$ as a function of [Cu^{II}] at pH 10 and 40 °C in the absence of Calmagite

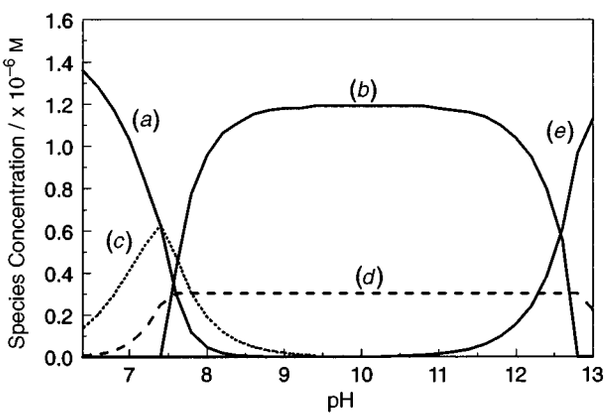

Fig. 6 Calculated speciation profile for 1.5×10^{-6} M Cu in the presence of 2.5×10^{-4} M $KHSO_5$ as a function of solution pH. Curves: (*a*) Cu^{II}; (*b*) $Cu(OH)_2$(ppt); (*c*) $[Cu(OH)]^+$; (*d*) $Cu(OH)_2$ and (*e*) $[Cu(OH)_3]^-$

Speciation calculations for the particular experimental conditions (Fig. 6) show that effectively all the Cu^{II} is present as $Cu(OH)_2$, thus Fig. 5 shows an apparent dependence on the concentration of $[Cu(OH)_2]^2$. Classically, of course, the activity of such a solid phase would be unity, so it is suggested that the dependence of the reaction upon the amount of precipitate is a consequence of reaction at its surface. We would not necessarily expect the surface area (or more accurately the surface area available for reacion) to vary linearly with the amount of copper hydroxide formed. In fact, the dependence on the square of copper hydroxide concentration suggests strongly that there is some form of limited poisoning of the surface, which is more critical for a low surface area than for a large one. In line with other studies[6] the observed rate exhibits a maximum at a pH equal to the pK_a of the peracid and the best fit to the data measured over the pH range from 9 to 10.5 is given by a rate expression of the form (17) where k is 6.1×10^{14} M^{-3} s^{-1}.

$$-d[KHSO_5]/dt = k[Cu(OH)_2]^2[SO_5^{2-}][HSO_5^-] \quad (17)$$

Poisoning is also observed at pH < 9, or, as we shall see later in the presence of dye, due to adsorption on $Cu(OH)_2$ particles.

A further twist is the observation that, if Cu^{II} is allowed to equilibrate in the presence of hydroxyl ions at pH 10 prior to reaction with $KHSO_5$, then the catalyst becomes inactive. This suggests that the active form of the catalyst is likely to be an initially formed, high-surface-area colloidal intermediate, or that morphology may be important. Clearly, much more work is necessary to pinpoint the precise nature of the active catalyst. Nevertheless, it is sufficient for kinetic analysis to identify the

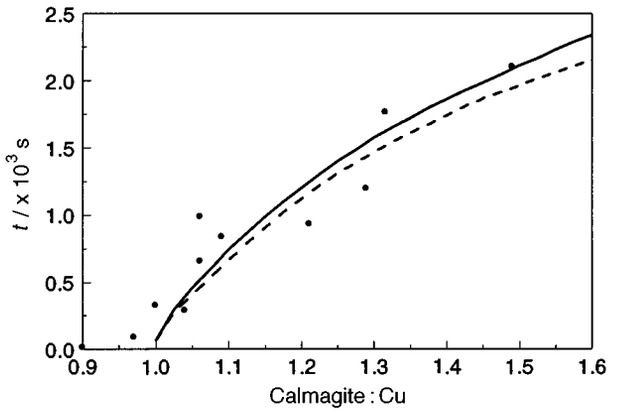

Fig. 7 Plot of observed induction time *versus* Calmagite : Cu ratio for the catalysed oxidation of Calmagite with 1×10^{-3} M $KHSO_5$ using 3.9×10^{-5} M Cu^{II} at pH 10 and 40 °C. The solid and broken curves are both theoretical fits, the former incorporating complexation with quinone reaction products

catalyst as $Cu(OH)_2$ and to have a mathematical expression for its catalytic action.

Independent studies of catalysed oxidation of a weakly complexing dye, Methyl Orange, in alkaline media produced a similar profile to that given in Fig. 5, revealing a similar order in [catalyst]. This suggests that both dye oxidation and peroxosulfate decomposition occur *via* a common catalytic intermediate. Speciation calculations modelling the conditions of catalysis at pH > 7 gave identical profiles to those in Fig. 6 and similarly suggest that the active catalyst is colloidal $Cu(OH)_2$.

The third area to investigate is the direct oxidation of [CuD] by peroxosulfate. It is known that Calmagite binds the copper ion very strongly.[2] When [D] > [Cu] the level of free copper ion in solution is of the order of 10^{-20} M. As 'free' Calmagite is oxidised by $KHSO_5$ the point is eventually reached where Calmagite and Cu^{II} are in equal concentrations. Beyond this point oxidation of [CuD] causes the 'free' copper(II) concentration to rise steeply, copper hydroxide precipitates and the rate of decolourisation dramatically and progressively increases. This effect is the origin of the induction period noted for these systems. It is relatively easy to measure this induction period by following the reaction with a spectrophotometer or by determining peracid profiles titrimetrically. This has been done for systems containing 3.93×10^{-5} M Cu^{II} and 1×10^{-3} M peroxosulfate with various levels of Calmagite at pH 10. The measured induction periods are plotted in Fig. 7 as a function of the Calmagite : copper ratio.

Thus, in addition to the non-catalysed oxidation of Calmagite [equations (14)–(16)] we must also quantify the reactions (18) and (19). The catalysed reaction will only occur when

direct oxidation of complexed dye

$$[CuD] + SO_5^{2-}/HSO_5^- \longrightarrow \text{products} + Cu(OH)_2 \quad (18)$$

catalysed oxidation of complexed dye

$$[CuD] + SO_5^{2-}/HSO_5^- \xrightarrow{Cu(OH)_2} \text{products} \quad (19)$$

copper hydroxide is present. If we run the finite difference model with the catalysed constant equal to zero when there is no precipitate of copper hydroxide and with some high value when copper hydroxide is present this will be sufficient to simulate an induction period. This allows us to use the model to determine the value for the rate constant for the uncatalysed decomposition of the [CuD] complex. Although direct oxidation of Calmagite occurs by electrophile attack by peracid,[10] oxidation of [CuD] can be simulated by assuming reaction occurs with the peracid nucleophile, probably *via* the metal centre as in earlier studies with manganese complexes.[1] The best

value is 0.155 M^{-1} s^{-1} and the corresponding theoretical fit of induction period against Calmagite : copper ratio is given in Fig. 7.

Comparison of the complexed and uncomplexed constants shows that complexing with copper ion protects the Calmagite against attack by peroxosulfate. The effect of including complexing by quinone products is to increase the induction time at higher Calmagite ratios as the quinone products complex copper ion and delay the onset of copper hydroxide precipitation. Including the binding of copper to quinone improves the fit to the experimental data in Fig. 7 over the whole range of Calmagite : copper ratios.

Finally, with the values of the rate constants determined so far it is possible to use the finite difference model to investigate the decolourisation of Calmagite by peroxosulfate in the presence of copper hydroxide precipitate. A number of possible schemes were tried but the best overall fit to the data was obtained with equation (20) where $k_1 = 4.2 \times 10^6$ and $k_2 = 3.51 \times$

$$-\mathrm{d[D]}/\mathrm{d}t = k_1[\mathrm{Cu(OH)_2}]^2[\mathrm{SO_5^{2-}}] + k_2[\mathrm{Cu(OH)_2}]^2[\mathrm{HSO_5^-}] \quad (20)$$

10^5 M^{-2} s^{-1}. This is zero order in [CuD] and implies a mechanism in which the [CuD] rapidly adsorbs to the copper hydroxide so that it saturates the available surface. The adsorbed [CuD] is then attacked by peroxosulfate. Attack by SO_5^{2-} proceeds faster than that by HSO_5^- although attack by both is required to fit the data over the whole pH range. Alternative schemes, which were rejected, were various combinations of rates that were first order in dye concentration or were of other orders in $[Cu(OH)_2]$ including zero and first order.

It was noticed that catalysed oxidant decomposition occurred at significantly higher $Cu(OH)_2$ levels in the presence of dye than in its absence. This suggests that adsorption of [CuD] on copper hydroxide particles inhibits catalysed oxidant decomposition. Adsorption of [CuD] also explains (*i*) the zero-order process in dye [equation (20)] and (*ii*) why sharp losses in $[KHSO_5]$ are only detected when the dye has been totally destroyed.

Comparison with experimental data

Comparison is made between theoretical predictions and experimental data in Fig. 3(*a*) and 3(*b*) for the autocatalytic step of the reaction [region (III)]. The figures depict changes in Calmagite absorbance for various $[D]_0$ as a function of time at pH 10; [Cu] and $[KHSO_5]$ were held constant at 6.3×10^{-5} and 5×10^{-4} M respectively. The fit is excellent at 6.83×10^{-5} and 5.6×10^{-5} M dye and, in view of the sensitivity of experimental rates to small changes in reactant concentrations, reasonably good at 4.55×10^{-5} M dye.

A similar comparison is given under conditions where the concentration of Cu^{II} approaches that of the dye [region (II)] in Fig. 2(*a*) and 2(*b*), and these also are in good agreement. The induction period, being the time elapsed before the fast reaction commences, is made up of two contributions, one proportional to the concentration of dye in excess of Cu^{II} (log D, a first-order process in D) and the other is related to [CuD]. Under the conditions of Fig. 2(*a*), where the bound dye concentration is fixed, the variation in the induction period is controlled by the excess dye concentration. The fits are not perfect, due to the extreme sensitivity to extraneous factors, but the model captures all the key features.

Three other comparisons were made, namely the influence of varying $[Cu^{II}]$ (Fig. 8), varying $[KHSO_5]$ (Fig. 9) and varying pH (Fig. 10). The latter deserves special mention as fits were possible only if it was assumed that attack is by both HSO_5^- and SO_5^{2-} with SO_5^{2-} being the more active species. Fig. 9 shows that the induction period is inversely proportional to $[KHSO_5]$, as anticipated from the rate law.

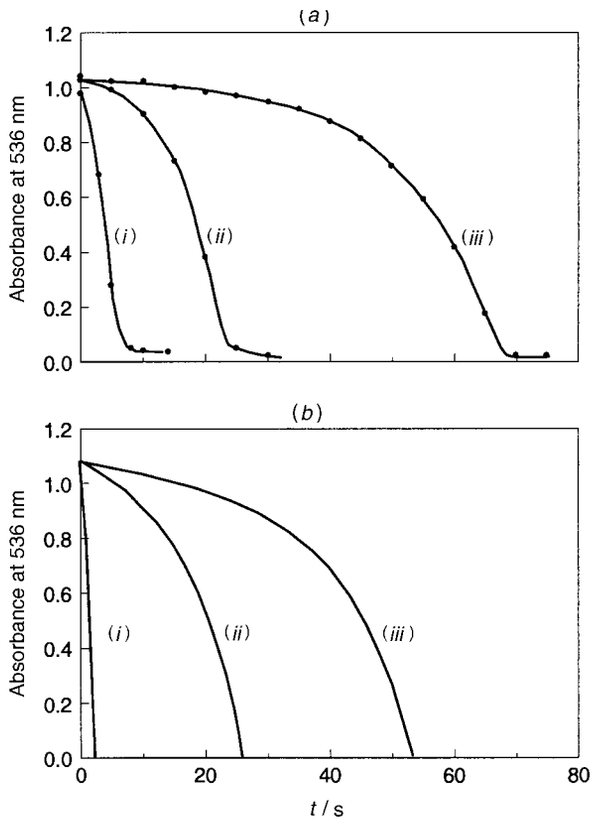

Fig. 8 (*a*) Influence of $[Cu^{II}]$ upon reaction profile for the catalysed oxidation of 4.5×10^{-5} M Calmagite with 5×10^{-4} M $KHSO_5$ at pH 10 and 40 °C. Curves (*i*) to (*iii*) represent 1.4×10^{-4}, 6.3×10^{-5} and 5.5×10^{-5} M Cu^{II} respectively. (*b*) Theoretical fits to the experimental data in (*a*)

It is illustrative to compute changes in various solution species as the reaction proceeds and this is conveniently represented in Fig. 11. This shows the oxidation of Calmagite and the role of the different ions and other species, as well as the catalysed oxidation proceeding through the various stages. The slow oxidation of the excess of free Calmagite in the original solution leads to a steep rise in the level of copper(II) ion as the 1 : 1 Cu : Calmagite equivalence point is reached. As [CuD] is oxidised $Cu(OH)_2$ precipitates and the catalysed oxidation begins. As more [CuD] is destroyed more $Cu(OH)_2$ is formed, leading to autocatalysis. These speciation profiles clearly indicate that the active catalyst is $Cu(OH)_2$ but the observation of zero-order kinetics in [D] suggests that the dye, in this case as [CuD], is closely associated with the catalyst surface. The profiles also indicate that [CuD] is catalytically inert.

Overall, the results are consistent with a mechanism in which a high-surface-area intermediate, formed during the precipitation of $Cu(OH)_2$, is the active catalyst. This appears to have a high affinity for the reactants and functions by increasing the effective reactant concentrations through rapid adsorption upon its surface.

Mechanistic insights

A number of key observations are listed below as they have important implications for the mechanism of catalysis.

(*i*) Catalysed $KHSO_5$ decomposition *and* catalysed dye oxidation show the same order in $[Cu(OH)_2]$, suggesting a common catalytic intermediate.

(*ii*) As described by equation (17), the observed second-order rate constant for catalysed $KHSO_5$ decomposition still has a maximum at its pK_a. The catalyst appears to function by facilitating high local concentrations of reactants *via* adsorption of the two negatively charged peroxosulfate species to its surface.

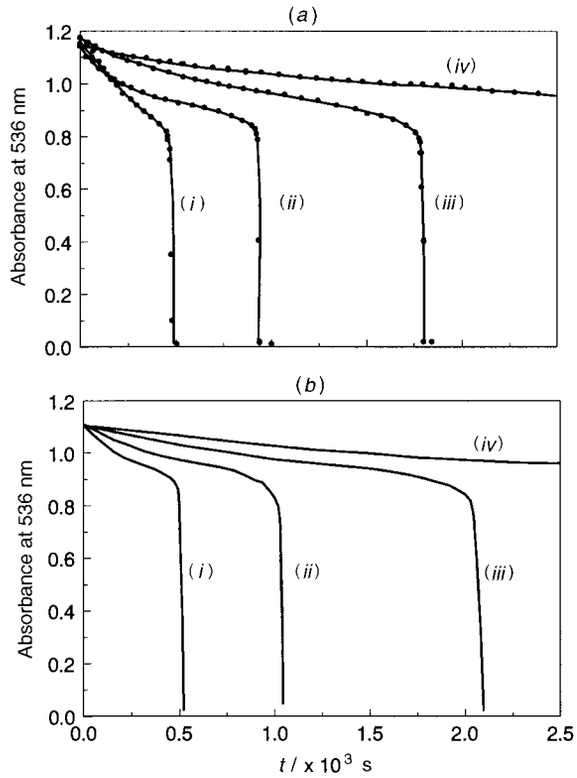

Fig. 9 (*a*) Influence of [$KHSO_5$] upon reaction profile for the catalysed oxidation of 5.2×10^{-5} M Calmagite using 3.9×10^{-5} M Cu^{II} at pH 10 and 40 °C. Curves (*i*) to (*iv*) represent [$KHSO_5$] = 4×10^{-3}, 2×10^{-3}, 1×10^{-3} and 0.5×10^{-3} M. (*b*) Theoretical fits to the experimental data in (*a*)

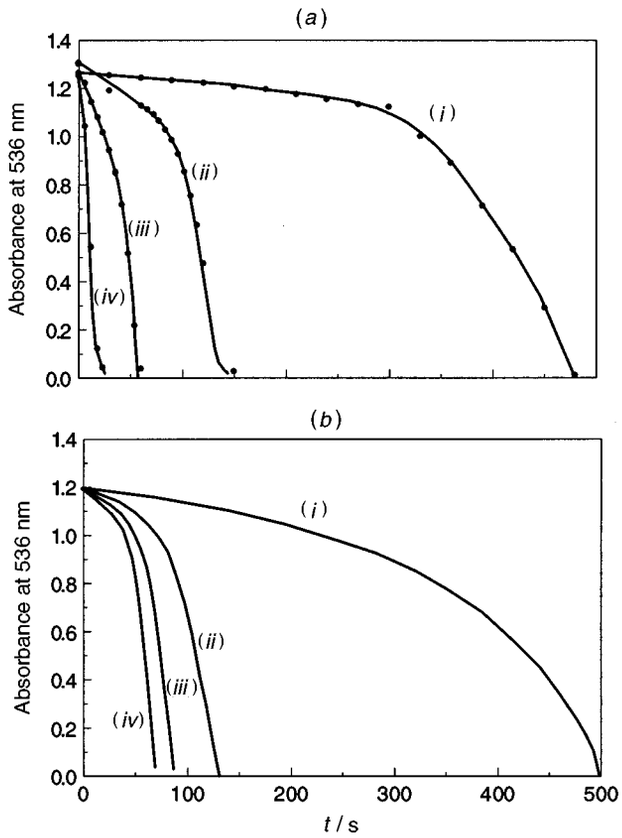

Fig. 10 (*a*) Influence of pH upon reaction profile for the catalysed oxidation of 5.6×10^{-5} M Calmagite with 5×10^{-4} M $KHSO_5$ using 6.3×10^{-5} M Cu^{II} at 40 °C. Curves (*i*) to (*iv*) correspond to pH 8.5, 9.5, 10 and 11 respectively. (*b*) Theoretical fits to the experimental data in (*a*)

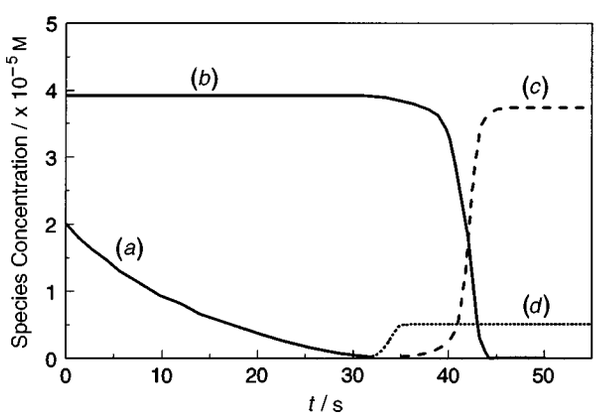

Fig. 11 Theoretical prediction of changes in the concentrations of copper and Calmagite species with extent of reaction for the catalysed oxidation of 5.8×10^{-5} M Calmagite with 1×10^{-3} M $KHSO_5$ using 3.9×10^{-5} M Cu^{II} at pH 10 and 40 °C. Curves (*a*) to (*d*) correspond to D, [CuD], $Cu(OH)_2$(ppt) and Cu^{II} respectively. Units are 10^{-5} M, except for [Cu^{II}] which has units 10^{-12} M. The various ion-pair species (Fig. 6) exhibit similar profiles to Cu^{II} and have concentrations $<10^{-7}$ M, so are omitted for simplicity.

(*iii*) The observation of zero-order kinetics in [CuD] indicates that this species is strongly adsorbed to the catalyst surface. When dye is added to an alkaline solution prepared from copper(II) salts a large shift is observed [11] in the copper(II) ESR spectrum, supporting the conclusion that dye can adsorb to copper hydroxide particles. Competitive adsorption of [CuD] with $KHSO_5$ species also explains why $KHSO_5$ decomposition is minimal in the presence of dye and why it accelerates when all the dye is oxidised.

(*iv*) Although dyes can be oxidised in the presence of an excess of Cu^{II} in alkaline media, abts [2,2′-azinobis(3-ethylbenzothiazoline-6-sulfonic acid) diammonium salt] is not. This suggests that a one-electron oxidation by oxidising radicals, *e.g.* hydroxyl radicals, does not occur [12] and, by elimination, that dye oxidation could be initiated by an oxygen-atom transfer step. Similarly, ESR studies with the common spin trap, dmpo (5,5-dimethyl-3,4-dihydropyrrole), did not give rise to a significant radical signal [13] in simple Cu–$KHSO_5$ systems.

(*v*) There is a complex rate dependence of both $KHSO_5$ decomposition and dye degradation on $[Cu(OH)_2]^2$ and an observed deviation at pH < 9 between experimental data and results calculated by equation (17). As these phenomena occur at low supersaturations, the reduction in catalytic activity is attributed to poisoning of the catalyst precipitation.

(*vi*) If Cu^{II} is allowed to equilibriate in alkaline media prior to addition of $KHSO_5$ then the catalyst is ineffective. This suggests that the specific nature of $Cu(OH)_2$ is a critical factor. Although this aspect is outside the scope of this paper, key factors may be the surface area of the catalyst and its morphology. Indeed, the catalyst $Cu(OH)_2$ actually exists as $CuO \cdot x$-H_2O *i.e.* hydrous copper in various states of hydration; in particular, its colour changes from pale blue to brown then to black as the pH is raised above 8.

Conclusion

The copper-catalysed peroxosulfate oxidation of Calmagite in alkaline media exhibits atypical kinetic profiles. The behaviour can be classified into three distinct regions: (*i*) when [Cu^{II}] ≪ [D] catalysis is ineffective so that 'free' dye *per se* is oxidised by $KHSO_5$; (*ii*) when [Cu^{II}] ≈ [D] all the copper is complexed and an induction period is observed; (*iii*) when [Cu^{II}] > [D] characteristic autocatalytic behaviour is observed.

A kinetic model, based upon independently generated constants and rate laws, has been derived which can predict changes in speciation with time and satisfactorily explain all the kinetic profiles. A key feature of the scheme is the rate-controlling direct oxidation of [CuD] by $KHSO_5$ to release Cu^{II}

in alkaline media; this, in turn, forms the active species, heterogeneous copper hydroxide, which results in autocatalytic dye destruction. The best fits are obtained assuming the catalytic step is first order in [SO_5^{2-}], *i.e.* peracid primarily acts as a nucleophile, and zero order in [CuD], *i.e.* bound dye adsorbs onto colloidal copper hydroxide.

Although its specific nature is unknown, chemical speciation calculations suggest that the active catalyst is a precipitated form of copper hydroxide, $Cu(OH)_2$. The catalyst appears to function by facilitating high local concentrations of reactants by adsorption of the two negatively charged peroxosulfate species to its surface.

Experimental

The main experimental details have been outlined previously.[1] The experimental work here differs in two major respects: (*i*) the need to minimise the influence of indigenous trace metals, which can catalyse oxidant decomposition or dye bleaching; (*ii*) the need to investigate copper-catalysed oxidant decomposition.

In kinetic studies featuring oxidising agents a sequestrant such as edta is normally added to obviate the influence of indigenous trace metals. Clearly, sequestrants need to be avoided in this investigation as they would complex Cu^{II} and interfere with catalysis. This presents some problems; first, systems devoid of metal sequestrant tend to give a variable background effect and hence a larger experimental error due to indigenous catalytic effects from trace metals, and secondly, where precipitation of copper hydroxide occurs in alkaline media (pH > 8.5), indigenous trace metals can influence ensuing nucleation and growth processes as they are known to induce flocculation of colloidal particles.[14]

Kinetic profiles were also found to be extremely sensitive to the precise ratio of Cu to D. As a consequence, extreme experimental care with regard to reagent concentrations was necessary. Experiments were thus conducted using preformed copper–Calmagite complexes, as this route gave the most reproducible results.

Copper sulfate (>99.5%) was obtained from BDH. Solution absorbances were followed at 536 nm, the absorption maximum of the [CuD] complex (molar absorption coefficient $\varepsilon = 2.4 \times 10^4$ M^{-1} cm^{-1}). Absorbances for the [CuD] complex obeyed the Beer–Lambert law over the range of interest (up to 1×10^{-4} M dye). There was no interference from product absorbances. Experiments were conducted under pseudo-first-order conditions, *i.e.* [peracid] ⩾ [D], but to achieve significant catalysis concentrations of catalyst of a similar magnitude to dye are required, *i.e.* $[Cu^{II}] \approx [D]$. Under conditions where there is an excess of ligand, the total absorbance was calculated from the molar absorption coefficient of Calmagite (1.3×10^4 at 536 nm and 2.0×10^4 M^{-1} cm^{-1} at 612 nm) and from that given above for [CuD].

The second-order rates for $KHSO_5$ decomposition were determined using standard iodometric techniques.[15] Observed second-order rate constants for the decomposition were determined from reciprocal concentration plots, *i.e.* 1/[$KHSO_5$] *vs.* time.

Finite difference model

The concept of finite difference is very simple. Complex reactive systems may typically have equilibria (which are rapidly established reversible reactions) as well as one or more slower non-reversible reactions. The finite difference method allows the simulation of such systems by proceeding in small time intervals adjusting concentrations of the various species at each time step. Provided the time step is small enough a very accurate representation can be given for even the most complex reaction scheme. However, the true power of the method lies in the ability to alter the representation of both reversible and irreversible reactions or the order of reactions very easily. This cannot easily be done with analytical solutions for such systems even supposing it is possible to derive them.

A Pentium personal computer with a Salford FORTRAN 77 Compiler was used to run the finite difference program, which was specifically written for the Cu–Calmagite–$KHSO_5$ system in FORTRAN. The method provides a tool for the investigation of the system as well as a complete model of it. The complete model was built in stepwise fashion beginning with measurements on simple components, progressing to binary mixtures and then to a complete description of the whole system. The code was validated at each step. Copies of the complete FORTRAN code are available on request.

The FORTRAN computer program allowed data input, performed the calculations and tabulated the results. It was used to try various combinations of constants and different reaction schemes. For example, in one form it scanned ranges of values of constants and picked the set giving the minimum deviation from the experimental data. When the analysis was complete this program had become, in effect, a computer model of the system.

As the model has many linked constants (kinetic, equilibrium, reaction order) it is difficult to specify the accuracy of any one constant. The test of our treatment, therefore, lies in the ability of the finished finite difference scheme to match the variation of the experimental measurements with component level and pH. For this reason we give a large number of such plots in order to allow the reader to judge the validity of the final result.

Acknowledgements

We thank Monica Garcia and Nigel Bird of this Laboratory for supplying their unpublished copper and dmpo ESR results, respectively. The contribution of Olive Laurie in determining catalysed $KHSO_5$ decomposition rate constants is gratefully acknowledged.

References

1 J. Oakes, P. L. Gratton and I. Weil, preceding paper.
2 A. E. Martell and R. M. Smith, *Critical Stability Constants*, Plenum, New York, 1977, vol. 3; L. G. Sillen and A. E. Martell, *Stability Constants—Supplement no. 1*, Special Publication 25, The Chemical Society, London, 1971.
3 F. A. Snavely, W. C. Ferneleus and B. E. Douglas, *J. Soc. Dyers Colour*, 1957, 73; F. A. Snavely and W. C. Ferneleus, *Science*, 1952, **15**, 117.
4 K. D. Karlin and Y. Gultneh, *Prog. Inorg. Chem.*, 1987, **35**, 219.
5 S. B. Brown, P. Jones and A. Suggett, *Inorganic Reaction Mechanisms*, ed. J. O. Edwards, Wiley, New York, 1970, 159; J. F. Goodman, P. Robinson and E. R. Wilson, *Trans. Faraday Soc.*, 1962, **58**, 1846.
6 D. L. Ball and J. O. Edwards, *J. Am. Chem. Soc.*, 1956, **78**, 1129.
7 S. Ooi, D. Carter and Q. Fernando, *Chem. Commun.*, 1967, 1301.
8 J. Crank, *The Kinetics of Diffusion*, Clarendon Press, Oxford, 2nd edn., 1975.
9 M. Chivukula, J. T. Spadaro and V. Rengenathan, *Biochemistry*, 1995, **34**, 7765; J. T. Spadaro and V. Rengenathan, *Arch. Biochem. Biophys.*, 1994, **312**, 301.
10 J. Oakes and P. L. Gratton, to be submitted.
11 R. Buchnall, Ph.D. Thesis, University of Sheffield, 1996; M. Garcia, unpublished work.
12 J. R. Lindsay-Smith, P. N. Balasubramanian and T. C. Bruice, *J. Am. Chem. Soc.*, 1988, **110**, 7411; S. L. Scott, W. Y. Chen, A. Bakac and J. H. Espenson, *J. Phys. Chem.*, 1993, **97**, 6710.
13 N. P. Bird, unpublished work.
14 R. J. Hunter, *Foundations of Colloid Science*, Oxford University Press, 1989, vol. 1, p. 395.
15 S. D. Sully and D. L. Williams, *Analyst* (*London*), 1962, **87**, 653; D. M. Davies and M. E. Deary, *Analyst* (*London*), 1988, **113**, 1473.

Received 21*st January* 1997; *Paper* 7/00481H